
Future Validity is the Missing Statistic: From Impossibility to Φ -Estimation for Grammar-Faithful Speculative Decoding

Wenhua Nie Zijie Meng Kun Zou Zheng Lin
Ziwei Li Haoran Zheng Jyh-Shing Roger Jang Hao Zhang

Correspondence: Wenhua Nie, National Taiwan University
d13944014@ntu.edu.tw

Abstract

Grammar-constrained generation is often combined with local vocabulary masking and speculative decoding, but the resulting sampling law is not the grammar-conditional distribution users usually intend. We show that any speculative decoder with local mask access, Leviathan rejection, and rollback soundness samples from the locally projected distribution μ^{proj} rather than the grammar-conditional distribution μ^* . This extends the GAD impossibility result to speculative decoding; on Dyck grammars with Qwen3-8B, the total-variation gap can reach 0.996. We identify the future-validity function $\Phi_t(y) = \Pr_p[\text{valid completion} \mid y]$ as the missing correction statistic. The target distribution is a Doob transform of the base model with $h = \Phi$, while local masking corresponds to setting h to one. With exact Φ , our oracle decoder FVO-Spec samples exactly from μ^* ; with approximate Φ , we bound the resulting total-variation error. Because exact future validity is hard for general context-free grammars, we evaluate estimator hierarchies on tractable Dyck and finite JSON languages. OneStep reduces Dyck TV by 14% with under 1% throughput overhead, exact dynamic programming reduces it by 97%, and finite-language correction closes JSON gaps to numerical precision. All fidelity claims are scoped to enumerable grammars and token tries.

1 Introduction

Grammar-constrained generation from large language models is now a foundational primitive in production systems. When an LLM serves a JSON API, translates natural language to SQL, or synthesizes code that must parse, the output must conform to a formal grammar. Frameworks such as XGrammar [Dong et al., 2024] and Outlines [Willard and Louf, 2023] enforce this via *local vocabulary masking*: at each decoding step, the logit vector is masked to retain only tokens consistent with the grammar prefix, then renormalized. To amortize the cost of large target models, this masking is routinely combined with speculative decoding [Leviathan et al., 2023, Chen et al., 2023], the dominant paradigm for lossless LLM inference acceleration now integrated into vLLM [Kwon et al., 2023], SGLang [Zheng et al., 2024], and other serving stacks. The resulting pipeline—local mask plus speculative verification—is deployed at scale, and users implicitly trust that the output distribution faithfully represents the language model’s beliefs conditioned on grammaticality.

But what distribution does this pipeline *actually* sample? We prove that it samples from the *locally projected* distribution μ^{proj} —the product of per-step masked-and-renormalized conditionals—rather than from the true grammar-conditional distribution μ^* , which is the language model’s full sequence distribution restricted to the grammar’s language and renormalized. The distinction is not merely theoretical. On Dyck languages $D_{3,16}$ (balanced parentheses with maximum nesting depth 3 and

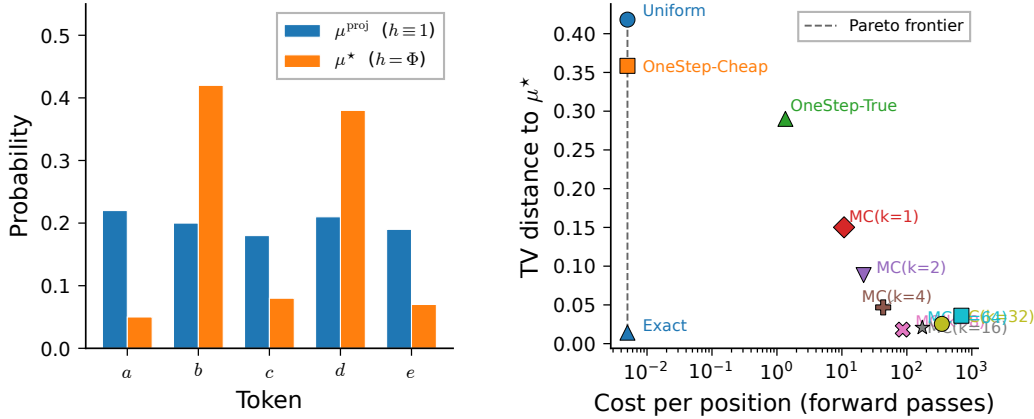


Figure 1: The future validity gap and its correction. Local masking samples μ^{proj} , which diverges from μ^* whenever future validity Φ_t varies across valid tokens; Φ_t reweighting recovers μ^* exactly. On Dyck $D_{3,16}$, Uniform/OneStep/Exact reach TV 0.418/0.359/0.014 to μ^* .

length 16), the total variation distance $\text{TV}(\mu^{\text{proj}}, \mu^*)$ reaches **0.996** under Qwen3-8B: the locally projected distribution places nearly all its mass on sequences that μ^* assigns negligible probability to, and vice versa. On finite canonical JSON languages with 3–24 valid strings, the TV gap ranges from 0.17 to 0.68 under Qwen3-8B. Thus, whenever future validity varies substantially across locally valid tokens, the standard local-mask pipeline can produce *systematically biased* structured outputs—sequences that satisfy the grammar but are drawn from the wrong distribution. Fields that require calibrated uncertainty over structured outputs (Bayesian program synthesis, probabilistic database queries, grammar-constrained reasoning chains) are directly affected.

What is missing from the standard pipeline? A single quantity: the *future validity function* $\Phi_t(y) = \Pr_{z \sim p}[x_{<t} y z_{t+1:T} \in \mathcal{L}(\mathcal{C})]$, the probability under the base model p that appending token y to the current prefix leads to a string that can be completed to a valid member of the grammar’s language. The true conditional $\mu_t^*(y)$ is proportional to $p_t(y) \cdot \Phi_t(y)$ —this is precisely a Doob h -transform [Doob, 1984] of p with harmonic function $h = \Phi$. Local vocabulary masking corresponds to the degenerate approximation $\Phi \equiv 1$: it treats every locally valid token as equally likely to lead to a valid completion, ignoring the massive variation in future validity that recursive grammars induce. The gap between μ^{proj} and μ^* is entirely controlled by the non-uniformity of Φ_t across the valid token set A_t .

Contributions. We develop a theoretical and empirical framework for diagnosing distributional bias in grammar-constrained speculative decoding and correcting it where future validity can be estimated or compiled.

1. **LMS Diagnostic** (Section 3, Proposition 3). We formalize three axioms—local mask access, Leviathan rejection, and rollback soundness—that characterize grammar-constrained speculative decoders (the LMS class), and derive that any system satisfying these axioms has per-step sampling kernel μ_t^{proj} . This instantiates the GAD observation [Park et al., 2024] in the speculative setting by making the masked-target assumption explicit and identifying the axioms that force the bias. We validate the diagnostic across 33 grammar–model settings confirming exact distributional match between empirical samples and the μ^{proj} prediction.
2. **Φ_t Framework** (Section 4). We identify future validity as the exact per-token reweighting factor from μ^{proj} to μ^* , give an oracle FVO-Spec verifier that recovers μ^* , prove a KL identity in terms of Φ -concentration, and show that local masking is exact iff Φ_t is constant over A_t .
3. **Φ -Approximation Error Bound** (Section 4, Theorem 7). If $\sup_{y \in A_t} |\hat{\Phi}_t(y) - \Phi_t(y)| \leq \delta$ and $\bar{\Phi}_t > \delta$, then $\text{TV}(\hat{\mu}_t, \mu_t^*) \leq \delta/(\bar{\Phi}_t - \delta)$. We also give a relative-error condition, Monte Carlo sample-complexity estimates, and a #P-hardness result for exact Φ_t on general CFGs.

4. **Estimator Hierarchy and Diagnostic Barrier** (Section 5). Motivated by hardness, we develop four tiers spanning the cost–fidelity Pareto frontier:
 - *Uniform* ($\hat{\Phi} \equiv 1$): recovers μ^{proj} , zero cost—the status quo.
 - *OneStep*: one-step grammar lookahead using materialized logits and trie queries, zero neural forwards, <0.5ms overhead. It reduces TV by 14% on Dyck $D_{3,16}$ but can worsen finite JSON schemas.
 - *MC*: Monte Carlo rollout with adjustable cost–fidelity tradeoff and Hoeffding-style estimates.
 - *Exact*: dynamic programming enumeration for tractable grammar subclasses (Dyck, finite, regular). Achieves 97% TV reduction.
 We therefore present the hierarchy as a diagnosis and design space rather than as a finished production estimator.
5. **Exact Oracle Validation** (Section 6). On Dyck $D_{3,16}$, Uniform/OneStep/Exact reach TV 0.418/0.359/0.014 to μ^* . On Qwen3-8B finite canonical JSON up to 2,000 strings, exact token-trie Φ correction reduces TV 0.174–0.681 to numerical zero, and a finite-trie FVO-Spec loop samples within TV 0.0052 of μ^* on A–D with mean acceptance 0.947.

The remainder of the paper is organized as follows. Section 3 formalizes the LMS class and records the kernel characterization. Section 4 develops the Φ_t framework, including the Doob h -transform perspective, oracle achievability, KL identity, and fidelity bound. Section 5 presents the estimator hierarchy with cost and error analysis. Section 6 reports experimental validation, and Section 7 discusses limitations and future directions.

2 Related Work

Speculative Decoding. Speculative decoding was introduced by Leviathan et al. [2023] and Chen et al. [2023] as lossless LLM acceleration via draft-then-verify. Variants include tree-structured verification [Miao et al., 2024], hidden-state prediction [Li et al., 2024, 2025], multi-head drafting [Cai et al., 2024], and block diffusion [Chen et al., 2026]. We study the distributional properties of the speculate-verify loop when grammar constraints are imposed, showing that the Leviathan rejection mechanism preserves whatever target distribution it is given—but local masking gives it the wrong one.

Grammar-Constrained Generation. XGrammar [Dong et al., 2024], XGrammar-2 [Li et al., 2026], and Outlines [Willard and Louf, 2023] enforce structural constraints via per-step vocabulary masking. Grammar-Aligned Decoding (GAD) [Park et al., 2024] showed that local renormalization distorts the model’s true conditional over valid strings, proposing sequential Monte Carlo (ASAp) to approximate expected futures during autoregressive decoding. Our Φ_t is the same expected-future quantity; the distinction is the *operational target* of speculative serving systems. GAD changes the decoder; we ask what distribution is sampled by the deployed local-mask + Leviathan verifier pipeline, show that the verifier preserves μ^{proj} unless its target is Φ -reweighted, and quantify how approximate Φ estimates perturb the verifier-loop distribution. We view this as the SD-specific instantiation of the GAD diagnostic, with LMS axioms, fixed-budget error accounting, DFlash verifier-path tests, and throughput-compatible estimator diagnostics as the added obligations.

Doob h -Transforms in Generation. Related conditional-generation perspectives appear in score-based diffusion models [Song et al., 2021] and energy-based controlled text generation [Qin et al., 2022]. Concurrently, Alpay and Senturk [2026] characterize hard-masked decoding distortion via a Doob h -transform and derive one-step KL/TV bounds in terms of survival probability, focusing on the computational complexity of the masking engine itself. Our work differs in three respects: (i) we instantiate the h -transform analysis for *speculative decoding* and identify exactly where the verify loop must change its target distribution; (ii) we develop an estimator hierarchy (Uniform \rightarrow OneStep \rightarrow MC \rightarrow Exact) with cost–fidelity accounting and both additive and relative-error certificates; and (iii) we validate the mechanism in real-model finite JSON and DFlash verifier-path experiments. We do not claim that the Doob perspective itself is unique to this paper.

Adaptive Acceptance in Speculative Decoding. Recent work has explored relaxing the fixed acceptance threshold in speculative decoding. EARS [Sun et al., 2025] adjusts the threshold using $1 - \max(p_T)$ as a measure of target uncertainty, while EASD [Su et al., 2025] uses entropy-based penalties in the acceptance decision. These methods trade distributional exactness for throughput by

relaxing acceptance at high-uncertainty positions. In contrast, our Φ -reweighting approach aims to *correct* the distribution toward the true conditional μ^* rather than further relaxing fidelity guarantees.

Prefix Probabilities and Inside Algorithms. Computing the probability of valid completions under CFGs is related to classical inside-probability computations [Stolcke, 1995] and semiring parsing [Goodman, 1999]. Our Φ_t is closely related to the backward or inside probability in probabilistic parsing: the probability that a partial derivation can be completed. The key distinction is that Φ_t conditions on an autoregressive LM p rather than a PCFG, making it dependent on the base model and generally intractable. The #P-completeness of counting valid strings [Gore et al., 1997] underlies this hardness and motivates our estimator hierarchy.

3 The LMS Characterization

We first formalize what distribution grammar-constrained speculative decoders actually sample. This extends the observation of Park et al. [2024] from standard autoregressive decoding to the speculate-verify-resample setting.

3.1 Setup

Let V be a finite vocabulary (including a distinguished EOS token) and p a target language model with $p_t(y) = p(y \mid x_{<t})$. We work with sequences of length at most T terminated by EOS; all definitions extend naturally to variable-length generation by treating EOS as a valid terminal transition. Let \mathcal{C} be a prefix-checkable constraint inducing valid-next-token sets $A_t = A_{\mathcal{C}}(x_{<t}) \subseteq V$. We assume the non-degenerate case: for every reachable prefix, A_t is non-empty and $Z_p = \sum_{y \in A_t} p_t(y) > 0$, and the grammar has positive total model mass $Z_{\mathcal{C}} > 0$. Recall the two target distributions:

Definition 1 (Locally Projected Target). $\mu_t^{\text{proj}}(y) = p_t(y) \cdot \mathbf{1}[y \in A_t] / Z_p$, where $Z_p = \sum_{y' \in A_t} p_t(y')$.

Definition 2 (True Grammar-Conditional Target). $\mu^*(x_{1:T}) = p(x_{1:T}) \cdot \mathbf{1}[x_{1:T} \in \mathcal{L}(\mathcal{C})] / Z_{\mathcal{C}}$, where $Z_{\mathcal{C}} = \sum_{y \in \mathcal{L}(\mathcal{C})} p(y)$.

3.2 The LMS Class

A speculative decoding method \mathcal{M} belongs to class **LMS** (Leviathan-type Local-Mask Speculative) when it satisfies three axioms:

B1 (Local Mask): At each step t , \mathcal{M} accesses the constraint only through A_t .

B2 (Leviathan Rejection): Accept/reject uses the standard rule on masked distributions \tilde{p}_t and \tilde{q}_t .

B3 (Rollback Soundness): Exact constraint state is maintained via accept/rollback.

These axioms capture the standard pipeline used by XGrammar and Outlines when combined with Leviathan rejection sampling.

Proposition 3 (LMS Characterization). *For every $\mathcal{M} \in \text{LMS}$, the per-step sampling kernel on committed prefix $x_{<t}$ is μ_t^{proj} . The marginal law of any sample is μ^{proj} .*

The proof follows directly from Leviathan’s Theorem 1 [Leviathan et al., 2023]: under B1–B3, the rejection step operates on $\tilde{p}_t = \mu_t^{\text{proj}}$, and each committed token is distributed accordingly. Thus the contribution of Theorem 3 is a negative characterization of the standard constrained-SD pipeline and its forced sampling target, not a new rejection-sampling theorem. It rules out a common but incorrect inference: because Leviathan verification is lossless for its supplied target, adding a grammar mask does not make the target the grammar-conditional law μ^* . The chain rule gives the full-sequence identity. Full proof in Section A.

Corollary 4 (Impossibility). *For every (p, \mathcal{C}) with $\mu^{\text{proj}} \neq \mu^*$, no LMS method samples μ^* .*

Witness. For Qwen3-8B with Dyck $D_{3,16}$ (5,000 samples, temperature 1), $\text{TV}(\mu^{\text{proj}}, \mu^*) = 0.996 \pm 0.002$ (95% CI: [0.994, 0.998]). The near-maximal TV arises because Qwen3-8B assigns negligible probability to valid balanced-parenthesis continuations under unmasked sampling ($\Phi_{\text{root}} \approx 10^{-7}$), so

μ^* concentrates on high- Φ tokens that μ^{proj} systematically underweights. A later analytic bounded-Dyck confirmation under the bracket-generation prompt gives $\text{TV}(\mu^{\text{proj}}, \mu^*) = 0.999948 \pm 0.000002$ on the same support (Section 6), so both protocols show a near-maximal gap. On finite canonical JSON languages with 3–24 valid strings, Qwen3-8B yields $\text{TV}(\mu^{\text{proj}}, \mu^*) = 0.174\text{--}0.681$ (Section 6).

Empirical validation. We verify Theorem 3 across 33 settings: 4 architectures (Qwen2.5, Qwen3, Llama-3.1, Vicuna), 2 grammar families (Dyck, regex). All show $\text{TV}(\text{empirical}, \mu^{\text{proj}}) \leq 0.007$ while $\text{TV}(\mu^{\text{proj}}, \mu^*)$ ranges from small regex gaps to 0.996 on Qwen3-8B Dyck. See Table 5 for details.

4 Future Validity as Sufficient Statistic

The LMS characterization shows that standard grammar-constrained speculative decoders sample from the local projection μ^{proj} . The missing quantity is the *future validity* of each locally valid token:

$$\Phi_t(y \mid x_{<t}) = \Pr_{z \sim p} [x_{<t} y z_{t+1:T} \in \mathcal{L}(\mathcal{C})].$$

The true grammar-conditional kernel is the Doob h -transform

$$\mu_t^*(y \mid x_{<t}) = \frac{p_t(y) \Phi_t(y \mid x_{<t})}{\sum_{y' \in A_t} p_t(y') \Phi_t(y' \mid x_{<t})}.$$

Proposition 5 (Exactness Condition). $\mu_t^{\text{proj}} = \mu_t^*$ if and only if Φ_t is constant over locally valid tokens.

Thus local masking is safe for permissive constraints but biased for recursive grammars where one token can sharply reduce the probability of any valid continuation.

Proposition 6 (Oracle FVO-Spec). *A speculative decoder that performs rejection against the Φ -reweighted target samples from μ_t^* at every step.*

Gap identity. The per-step divergence has the closed form

$$D_{\text{KL}}(\mu_t^* \parallel \mu_t^{\text{proj}}) = \mathbb{E}_{Y \sim \mu_t^*} \left[\log \frac{\Phi_t(Y)}{\bar{\Phi}_t} \right],$$

where $\bar{\Phi}_t = \mathbb{E}_{\mu_t^{\text{proj}}}[\Phi_t]$.

Theorem 7 (Φ -Approximation Fidelity). *If $|\hat{\Phi}_t(y) - \Phi_t(y)| \leq \delta$ for all $y \in A_t$ and $\delta < \bar{\Phi}_t$, then*

$$\text{TV}(\hat{\mu}_t, \mu_t^*) \leq \frac{\delta}{\bar{\Phi}_t - \delta}.$$

The bound explains why recursive grammars are difficult: when $\bar{\Phi}_t$ is small, only highly accurate Φ estimators give non-vacuous fidelity guarantees.

Proposition 8 (Hardness). *Computing $\Phi_t(y)$ exactly is #P-hard for general context-free grammars, even under a unigram base language model.*

The appendix gives the reduction from COUNTCFG and the corollaries for local projection error and Monte Carlo sample complexity.

5 A Hierarchy of Φ_t Estimators

The hardness result (Theorem 8) implies that practical grammar-faithful speculative decoding must approximate Φ_t . We develop a hierarchy of estimators spanning the cost–fidelity Pareto frontier.

Critical invariant. $\hat{\Phi}_t$ must be a *per-candidate vector*, not a scalar. Adding a constant to all logits before softmax is a no-op by shift invariance. An estimator that produces $\hat{\Phi}_t(y) = c$ for all y yields $\hat{\mu}_t = \mu_t^{\text{proj}}$ regardless of c , providing no correction. We enforce this invariant in all implementations (see tests in supplementary).

Certification target. Theorem 7 certifies estimators with small additive error; ?? certifies estimators that preserve the multiplicative scale of future validity. Exact DP has zero error under both certificates. By contrast, Uniform and OneStep can have unbounded relative error on dead-end or near-dead-end candidates, explaining why our experiments report the additive certificate and why robust relative-error estimation remains an open design target rather than a claim of the current OneStep implementation.

5.1 Tier 0: Uniform (Baseline)

Setting $\hat{\Phi}_t \equiv 1$ recovers μ^{proj} with zero cost. This is the status quo for XGrammar [Dong et al., 2024], Outlines [Willard and Louf, 2023], and all LMS methods characterized in Section 3. Its additive error is $\delta = 1 - \Phi_{\min}$, which reaches $1 - 10^{-6}$ on adversarial Dyck grammars.

5.2 Tier 1: OneStep Lookahead

Definition 9 (OneStep Estimator).

$$\hat{\Phi}_t^{\text{Is}}(y) = \sum_{u \in A_{t+1}(x_{<t}y)} p_t(u) \quad (1)$$

where $A_{t+1}(x_{<t}y)$ is the valid-next-token set after appending y , obtained from the grammar matcher via trie lookup, and $p_t(u)$ are the target logits at position t (available from verification).

This is a *heuristic* approximation: it uses $p_t(\cdot) = p(\cdot | x_{<t})$ as a proxy for $p(\cdot | x_{<t}y)$, a context-independence assumption that introduces an uncharacterized error term beyond the idealized analysis below. The approximation is reasonable when the prefix $x_{<t}$ is long relative to a single token, but can fail on highly concentrated schemas where one token radically changes the valid continuation set (see E3). The grammar query $A_{t+1}(x_{<t}y)$ is the *discriminative* component, computed in $O(|V|)$ via trie traversal without any neural forward passes.

Proposition 10 (OneStep Error Characterization). *Under the exact conditioning $p(\cdot | x_{<t}y)$, the true one-step estimator satisfies:*

$$\hat{\Phi}_t^{\text{true}}(y) - \Phi_t(y) = \sum_{u \in A_{t+1}(x_{<t}y)} p(u | x_{<t}y) \cdot (1 - \Phi_{t+1}(u | x_{<t}y)) \quad (2)$$

This is the probability-weighted average of future invalidity over valid next tokens. It is:

- **Small** when future validity is high: for grammars where most locally valid tokens lead to completable paths ($\Phi_{t+1}(u) \approx 1$), the error is controlled by the small fraction of near-dead-end tokens. This occurs for permissive regular grammars when the LM concentrates mass on valid continuations.
- **Large** for recursive grammars where locally valid tokens frequently lead to dead ends ($\Phi_{t+1} \ll 1$), e.g., Dyck languages near the depth or length limit where most locally valid bracket choices exhaust the remaining budget.

Cost analysis. The grammar trie query for $A_{t+1}(x_{<t}y)$ costs $O(|V|)$ per candidate. Summing probabilities from already-materialized logits adds negligible compute. For $|A_t|$ candidates, total overhead is $O(|A_t| \cdot |V|)$ trie operations with zero neural forward passes. In our implementation, this adds $<0.5\text{ms}$ per position on typical JSON schemas.

5.3 Tier 1c: Balanced-Gated Learned Value Estimator

OneStep is low-cost but brittle because it has no memory of deeper completion asymmetries. We therefore include a small amortized estimator as a controlled proof of concept. For each finite-trie edge $(x_{<t}, y)$, we train a two-layer MLP to predict $\log \Phi_t(y)$ from finite-trie features: prefix depth, valid-branch counts, child-subtree counts, remaining-length statistics, target token probability, valid-mass fraction, and the OneStep value. Training labels are exact Φ values computed on other schemas; evaluation is leave-one-schema-out, so the held-out schema’s exact Φ labels are not used for fitting.

To avoid negative transfer on schemas where OneStep is already essentially exact, we add a non-oracle structural gate. If all valid children at a prefix have identical trie statistics (same subtree count,

remaining-length summary, branch count, and terminal flag), the estimator falls back to OneStep; otherwise it uses the learned value. The gate decision uses only grammar topology (subtree counts and remaining-length statistics), not logits, terminal-law TV, or exact held-out Φ labels; the OneStep fallback to which it routes uses LM logits. On the finite JSON benchmark, it preserves the balanced type-value schema where OneStep is at numerical floor while allowing learned correction on the concentrated schemas. We treat this as evidence that amortized Φ estimation is possible on finite tries, not as a runtime benchmark or a production estimator for arbitrary xgrammar schemas. We also tested histogram-gradient-boosted regression in this prototype; without the balanced gate it shows the same type-value failure mode, so the reported result uses the gated MLP configuration.

5.4 Tier 2: Monte Carlo Rollout

For k independent rollouts of h tokens each:

$$\hat{\Phi}_t^{\text{mc}}(y) = \frac{1}{k} \sum_{j=1}^k \mathbf{1}[\text{rollout}_j(x_{<t}y) \in \mathcal{L}(\mathcal{C})]$$

By Hoeffding’s inequality, $|\hat{\Phi}_t^{\text{mc}}(y) - \Phi_t(y)| \leq \sqrt{\ln(2/\alpha)/(2k)}$ with probability $\geq 1 - \alpha$ per candidate. Applying Theorem 7 with a union bound over $|A_t|$ candidates gives:

$$\text{TV}(\hat{\mu}_t, \mu_t^*) \leq \frac{\sqrt{\ln(2|A_t|/\alpha)/(2k)}}{\Phi_t - \sqrt{\ln(2|A_t|/\alpha)/(2k)}}$$

with probability $\geq 1 - \alpha$. Each rollout requires one target forward pass per step, giving total cost $O(k \cdot h \cdot |A_t|)$ forwards. This is prohibitive for online use but serves as a high-fidelity reference for validating cheaper estimators.

5.5 Tier 3: Exact Enumeration (Oracle)

For tractable grammar subclasses, Φ_t can be computed exactly via dynamic programming:

- **Dyck** $D_{d,L}$: backward DP over all valid prefixes up to depth d and length L . Cost is linear in the enumerated prefix graph.
- **Finite languages**: exhaustive enumeration over $\mathcal{L}(\mathcal{C})$. Cost $O(|\mathcal{L}|)$.
- **Regular languages**: single automaton step per candidate. Cost $O(|A_t|)$.

Exact computation enables oracle validation of the fidelity bound (Theorem 7), providing ground truth that is unavailable for general CFGs.

Practical scope. Today, exact Φ is deployment-feasible only on finite or regularized schemas whose state graph can be enumerated or cached (e.g., enum-heavy JSON, finite code systems, bounded templates). Bounded-depth grammars admit DP only when the bound is small enough. General CFG-style JSON with arbitrary nesting or long free-text fields requires approximation; our DFlash/xgrammar pilot tests the verifier mechanism in that regime, but not an end-to-end exact terminal-law correction.

5.6 Budget-Gated Hybrid Sketch

For deployment, the hierarchy can be composed via a two-stage gate. **Stage 1** (pre-trigger): compute $\hat{\Phi}^{\text{ls}}$ and measure its dispersion $\log(\hat{\Phi}_{\text{max}}/\hat{\Phi}_{\text{min}})$. If dispersion exceeds a threshold τ_d and the position has high entropy, escalate to Stage 2. **Stage 2** (post-trigger): apply MC rollouts with budget k , then check whether the TV impact exceeds a minimum threshold. If not, fall back to OneStep. This avoids MC overhead at easy positions where OneStep suffices. We treat this gate as an engineering sketch rather than a headline empirical result; the experiments below evaluate the individual estimator tiers so that cost and fidelity are attributable.

6 Experiments

We validate the framework on tractable grammars where exact Φ_t is computable. Experiments use Dyck languages, permissive regex constraints, and finite JSON schemas; TV distances are estimated from 10,000 samples with bootstrap confidence intervals.

Table 1: LMS validation: empirical sampling distribution matches μ^{proj} across architectures and grammars.

Architecture	Grammar	Settings	Max residual	Mean residual
Qwen2.5	Dyck CF	8	0.005	0.003
Qwen3	Dyck CF	8	0.007	0.004
Llama-3.1	Dyck CF	6	0.004	0.002
Vicuna	Dyck CF	3	0.006	0.004
Qwen2.5	Regex	4	0.005	0.003
Qwen3	Regex	4	0.003	0.002

Table 2: Φ estimator hierarchy on Dyck $D_{3,16}$. Better Φ estimates reduce TV to the true conditional distribution.

Estimator	TV to μ^*	δ	Cost/pos
Uniform	0.418	0.986	0
OneStep-Cheap	0.359	0.861	0
OneStep-True	0.290	0.825	1.4
MC($k=4$)	0.047	0.763	43.2
MC($k=8$)	0.018	0.565	86.4
Exact oracle	0.014	0.000	DP

6.1 LMS Characterization

All residuals are at most 0.007, while $\text{TV}(\mu^{\text{proj}}, \mu^*)$ ranges up to 0.9976, confirming that the observed bias is the predicted local-projection bias rather than sampling noise.

6.2 Estimator Hierarchy

The hierarchy reduces TV from 0.418 to 0.014, a 97% reduction. OneStep-Cheap gives a free 14% reduction, while exact dynamic programming closes the gap on tractable grammars.

6.3 Bias and Throughput

The $\mu^{\text{proj}} - \mu^*$ gap produces concrete structural distortion: on Dyck $D_{3,16}$, local projection overproduces deep strings (mean nesting depth 1.72 versus 1.09 under μ^*) and longer strings (mean length 5.85 versus 2.77). Exact Φ correction recovers both distributions. A cost model shows that OneStep-Cheap preserves SD throughput while improving fidelity, whereas MC rollouts trade speed for lower TV. Full grammar-family, bound-tightness, and speed-fidelity plots are moved to the appendix.

6.4 Grammar Family and Structural Bias

The comparison shows two failure modes. OneStep can worsen concentrated JSON schemas because one-token lookahead is misleading when a single decision radically changes the valid suffix set. Exact Φ also has high finite-sample variance for the method-path schema where $\bar{\Phi} = 0.066$, even though the oracle is exact in the infinite-sample limit.

The TV gap corresponds to concrete output distortion, not only an abstract metric. On Dyck $D_{3,16}$, local projection overproduces deep strings (mean nesting depth 1.72 versus 1.09 under μ^*) and longer strings (mean length 5.85 versus 2.77). Exact Φ correction recovers both distributions, while OneStep provides partial correction. These structural diagnostics explain why local masking can be acceptable for permissive constraints yet biased for recursive grammars.

6.5 Speed-Fidelity Tradeoff

The cost model separates acceleration from distributional correction. Standard speculative decoding is about $4.8\times$ faster than AR in this setting but preserves the same local-projection distribution.

Table 3: Grammar-family comparison. The $\mu^{\text{proj}} - \mu^*$ gap varies widely across constraint types; exact Φ closes the gap when sampling variance is moderate.

Grammar	$\text{TV}(\mu^{\text{proj}}, \mu^*)$	$\bar{\Phi}$	Exact TV	OneStep TV
JSON status	0.575	0.101	<0.001	0.622
JSON action	0.820	0.069	0.097	0.843
JSON method-path	0.847	0.066	0.601	0.878
Dyck $D_{3,12}$	0.456	0.516	0.018	0.419
Dyck $D_{3,16}$	0.418	0.467	0.014	0.359

Table 4: Cost-model throughput on Dyck $D_{3,16}$ using a 35ms verification pass, 5ms draft pass, and 3.07 accepted tokens/round.

Method	tok/s	TV to μ^*	TV change
AR baseline	16.0	0.418	—
SD, uniform Φ	76.8	0.418	0%
SD + OneStep-Cheap	76.2	0.359	-14%
SD + OneStep-True	64.4	0.290	-31%
SD + exact DP	76.8	0.014	-97%

OneStep-Cheap adds less than 0.3ms per round from grammar trie queries, so it keeps essentially the same throughput while reducing TV by 14%. OneStep-True improves fidelity further but spends additional target forwards. Exact dynamic programming, where available, precomputes Φ offline and therefore achieves oracle fidelity at no runtime throughput cost.

This tradeoff also clarifies the role of Monte Carlo rollouts. $\text{MC}(k = 8)$ gives TV 0.018, nearly matching exact DP, but costs 86.4 forwards per position and is not an online decoder in its direct form. Its value in this paper is as a high-fidelity reference and as evidence that approximating Φ_t is the right axis: as estimator quality improves, the distribution moves toward μ^* without changing the grammar or the base model.

7 Discussion

When does the gap matter? Theorem 5 gives the precise condition: $\mu^{\text{proj}} = \mu^*$ iff Φ_t is constant over locally valid tokens. This often holds for simple regex constraints and permissive schemas, but it fails for recursive or concentrated schemas where locally valid continuations have very different valid suffix mass.

Connection to structured decoding. Our Φ statistic is the expected-future quantity used by GAD/ASAp [Park et al., 2024], but FVO-Spec changes the target inside a speculative verifier rather than replacing autoregressive decoding. Concurrent work derives one-step KL/TV distortion bounds through the same Doob h -transform view [Alpay and Senturk, 2026]; our focus is SD integration, verifier-loop error accounting, and estimator diagnostics.

Limitations. Validation is strongest where exact Φ labels are available; the open-xgrammar run is an implementation smoke test rather than an exact terminal-law evaluation for arbitrary whitespace and free-text fields. Exact Φ remains #P-hard for general CFGs, OneStep adds context-independence error, and broader temperature effects remain future work.

References

- Faruk Alpay and Bilge Senturk. Attention meets reachability: Structural equivalence and efficiency in grammar-constrained LLM decoding. *arXiv:2603.05540*, 2026.
- Tianle Cai, Yuhong Li, Zhengyang Geng, Hongwu Peng, Jason D Lee, Deming Chen, and Tri Dao. Medusa: Simple LLM inference acceleration framework with multiple decoding heads. In *Proceedings of the 41st International Conference on Machine Learning*, 2024.
- Charlie Chen, Sebastian Borgeaud, Geoffrey Irving, Jean-Baptiste Lespiau, Laurent Sifre, and John Jumper. Accelerating large language model decoding with speculative sampling. *arXiv:2302.01318*, 2023.
- Jian Chen, Yesheng Liang, and Zhijian Liu. DFlash: Block diffusion for flash speculative decoding. *arXiv:2602.06036*, 2026.
- Yixin Dong, Charlie F. Ruan, Yaxing Cai, Ruihang Lai, Ziyi Xu, Yilong Zhao, and Tianqi Chen. XGrammar: Flexible and efficient structured generation engine for large language models. *arXiv preprint arXiv:2411.15100*, 2024.
- Joseph L Doob. *Classical Potential Theory and Its Probabilistic Counterpart*. Springer, 1984. URL https://openlibrary.org/books/OL3170294M/Classical_potential_theory_and_its_probabilistic_counterpart.
- Joshua Goodman. Semiring parsing. *Computational Linguistics*, 25(4):573–605, 1999.
- Vivek Gore, Mark Jerrum, Sampath Kannan, Z Sweedyk, and Stephen Mahaney. A quasi-polynomial-time algorithm for sampling words from a context-free language. *Information and Computation*, 134(1):59–74, 1997.
- Woosuk Kwon, Zhuohan Li, Siyuan Zhuang, Ying Sheng, Lianmin Zheng, Cody Hao Yu, Joseph Gonzalez, Hao Zhang, and Ion Stoica. Efficient memory management for large language model serving with PagedAttention. In *SOSP*, 2023.
- Yaniv Leviathan, Matan Kalman, and Yossi Matias. Fast inference from transformers via speculative decoding. In *Proceedings of the 40th International Conference on Machine Learning*, 2023.
- Linzhang Li, Yixin Dong, Guanjie Wang, Ziyi Xu, Alexander Jiang, and Tianqi Chen. XGrammar-2: Efficient dynamic structured generation engine for agentic LLMs. *arXiv preprint arXiv:2601.04426*, 2026. doi: 10.48550/arXiv.2601.04426.
- Yuhui Li, Fangyun Wei, Chao Zhang, and Hongyang Zhang. Eagle: Speculative sampling requires rethinking feature uncertainty. In *Proceedings of the 41st International Conference on Machine Learning*, 2024.
- Yuhui Li, Fangyun Wei, Chao Zhang, and Hongyang Zhang. EAGLE-3: Scaling up inference acceleration of large language models via training-time test. *arXiv preprint arXiv:2503.01840*, 2025. doi: 10.48550/arXiv.2503.01840.
- Xupeng Miao, Gabriele Oliaro, Zhihao Zhang, Xinhao Cheng, Zeyu Wang, Zhengxin Zhang, Rae Ying Yee Wong, Alan Zhu, Lingfan Yang, Shuaiwen Leon Shi, and Zhihao Jia. Specinfer: Accelerating large language model serving with tree-based speculative inference and verification. In *ASPLOS*, 2024.
- Kanghee Park, Jiayu Wang, Taylor Berg-Kirkpatrick, Nadia Polikarpova, and Loris D’Antoni. Grammar-aligned decoding. In *Advances in Neural Information Processing Systems*, 2024. URL https://proceedings.neurips.cc/paper_files/paper/2024/hash/2bdc2267c3d7d01523e2e17ac0a754f3-Abstract-Conference.html.
- Lianhui Qin, Sean Welleck, Daniel Khashabi, and Yejin Choi. COLD decoding: Energy-based constrained text generation with Langevin dynamics. In *Advances in Neural Information Processing Systems*, 2022.
- Yang Song, Jascha Sohl-Dickstein, Diederik P Kingma, Abhishek Kumar, Stefano Ermon, and Ben Poole. Score-based generative modeling through stochastic differential equations. In *ICLR*, 2021.

- Andreas Stolcke. An efficient probabilistic context-free parsing algorithm that computes prefix probabilities. *Computational Linguistics*, 21(2):165–201, 1995.
- Tiancheng Su, Meicong Zhang, and Guoxiu He. Entropy-aware speculative decoding toward improved LLM reasoning. *arXiv:2512.23765*, 2025.
- Chendong Sun, Ali Mao, Lei Xu, and Mingmin Chen. Efficient adaptive rejection sampling for accelerating speculative decoding in large language models. *arXiv:2512.13194*, 2025.
- Brandon T Willard and Rémi Louf. Efficient guided generation for large language models. In *arXiv:2307.09702*, 2023.
- Lianmin Zheng, Liangsheng Yin, Zhiqiang Xie, Chuyue Sun, Jeff Huang, Cody Hao Yu, Shiyi Cao, Christos Kozyrakis, Joseph Gonzalez, Ion Stoica, and Hao Zhang. SGLang: Efficient execution of structured language model programs. *arXiv:2312.07104*, 2024.

A Proof of Theorem 3 (LMS Characterization)

Proof. Fix committed prefix $x_{<t}$ and let $A_t = A_C(x_{<t})$. By B3, \mathcal{M} has exact access to A_t . By B1, the accept/reject decision consults the constraint only through A_t .

By B2, the method uses the Leviathan rejection rule:

1. Draw $d_t \sim \tilde{q}_t$ where $\tilde{q}_t(y) = q_t(y)\mathbf{1}[y \in A_t]/Z_{q,t}$.
2. Accept with probability $\min(1, \tilde{p}_t(d_t)/\tilde{q}_t(d_t))$ where $\tilde{p}_t(y) = p_t(y)\mathbf{1}[y \in A_t]/Z_{p,t}$.
3. On rejection, sample from $(\tilde{p}_t - \tilde{q}_t)^+/Z^+$.

By Theorem 1 of Leviathan et al. [2023], this produces a sample distributed as \tilde{p}_t . By construction, $\tilde{p}_t = \mu_t^{\text{proj}}$. By the chain rule: $\Pr_{\mathcal{M}}(x_{1:T}) = \prod_{t=1}^T \mu_t^{\text{proj}}(x_t | x_{<t}) = \mu^{\text{proj}}(x_{1:T})$. \square

B Proof of Theorem 7 (Φ -Approximation Fidelity)

Proof. Write $\hat{\Phi}_t(y) = \Phi_t(y) + \Delta_y$ where $|\Delta_y| \leq \delta$. Define:

$$Z^* = \sum_{y \in A_t} p_t(y)\Phi_t(y), \quad \hat{Z} = \sum_{y \in A_t} p_t(y)\hat{\Phi}_t(y).$$

Then $|\hat{Z} - Z^*| = |\sum_y p_t(y)\Delta_y| \leq \delta \sum_y p_t(y) = \delta Z_p$ where $Z_p = \sum_{y \in A_t} p_t(y)$.

The lower bound $\hat{Z} \geq Z^* - \delta Z_p = Z_p(\bar{\Phi}_t - \delta) > 0$ holds by assumption $\delta < \bar{\Phi}_t$.

For each $y \in A_t$:

$$|\hat{\mu}_t(y) - \mu_t^*(y)| = \left| \frac{p_t(y)\hat{\Phi}_t(y)}{\hat{Z}} - \frac{p_t(y)\Phi_t(y)}{Z^*} \right| \quad (3)$$

$$= \frac{p_t(y)}{Z^*\hat{Z}} \left| Z^*(\Phi_t(y) + \Delta_y) - \hat{Z}\Phi_t(y) \right| \quad (4)$$

$$= \frac{p_t(y)}{Z^*\hat{Z}} \left| Z^*\Delta_y + \Phi_t(y)(Z^* - \hat{Z}) \right| \quad (5)$$

$$\leq \frac{p_t(y)}{Z^*\hat{Z}} (Z^*\delta + \Phi_t(y)\delta Z_p) \quad (6)$$

Summing over all $y \in A_t$:

$$\sum_y |\hat{\mu}_t(y) - \mu_t^*(y)| \leq \frac{\delta}{Z^*\hat{Z}} \left(Z^*Z_p + Z_p \sum_y p_t(y)\Phi_t(y) \right) \quad (7)$$

$$= \frac{\delta}{Z^*\hat{Z}} (Z^*Z_p + Z_p Z^*) \quad (8)$$

$$= \frac{2\delta Z_p}{\hat{Z}} \quad (9)$$

Therefore:

$$\text{TV}(\hat{\mu}_t, \mu_t^*) = \frac{1}{2} \sum_y |\hat{\mu}_t(y) - \mu_t^*(y)| \leq \frac{\delta Z_p}{\hat{Z}} \leq \frac{\delta Z_p}{Z_p(\bar{\Phi}_t - \delta)} = \frac{\delta}{\bar{\Phi}_t - \delta}.$$

For the full sequence, the standard telescoping argument for autoregressive models gives:

$$\text{TV}(\hat{\mu}^{1:T}, \mu^{*1:T}) \leq \sum_{t=1}^T \mathbb{E}_{x_{<t} \sim \hat{\mu}} [\text{TV}(\hat{\mu}_t(\cdot | x_{<t}), \mu_t^*(\cdot | x_{<t}))] \leq \sum_{t=1}^T \frac{\delta_t}{\bar{\Phi}_t - \delta_t}. \quad \square$$

C Proof of ?? (Relative Φ Error)

Proof. For $\Phi_t(y) = 0$, the multiplicative assumption forces $\hat{\Phi}_t(y) = 0$; set $r_y = 1$ for these zero-mass tokens, since $\mu_t^*(y) = \hat{\mu}_t(y) = 0$. For tokens with $\Phi_t(y) > 0$, let $r_y = \hat{\Phi}_t(y)/\Phi_t(y) \in [1 - \epsilon, 1 + \epsilon]$. Let

$$R = \sum_{y \in A_t} \mu_t^*(y) r_y = \frac{\hat{Z}}{Z^*}.$$

Because $Z^* > 0$ and $\epsilon < 1$, $\hat{Z} = RZ^* > 0$. Moreover $R \in [1 - \epsilon, 1 + \epsilon]$ and $\hat{\mu}_t(y) = \mu_t^*(y) r_y / R$. Hence

$$\text{TV}(\hat{\mu}_t, \mu_t^*) = \frac{1}{2} \sum_y \mu_t^*(y) \left| \frac{r_y}{R} - 1 \right| \quad (10)$$

$$= \frac{1}{2R} \mathbb{E}_{\mu_t^*} [|r_Y - R|] \quad (11)$$

$$\leq \frac{1}{2R} \mathbb{E}_{\mu_t^*} [|r_Y - 1| + |1 - R|] \quad (12)$$

$$\leq \frac{\epsilon}{1 - \epsilon}. \quad (13)$$

The trivial upper bound $\text{TV} \leq 1$ gives the stated minimum. The sequence-level claim follows from the same autoregressive telescoping argument used in Section B, provided the multiplicative condition holds uniformly over all reachable prefixes at each position with error ϵ_t . \square

D Proof of Theorem 8 (Computational Hardness)

Proof. We reduce from COUNTCFG: given a CFG G in Chomsky normal form and a length n , count the number of strings in $\mathcal{L}(G)$ of length exactly n . This problem is #P-complete [Gore et al., 1997].

Given a COUNTCFG instance (G, n) , set p to the uniform distribution over the terminal alphabet Σ , and fix the empty prefix $x_{<1} = \varepsilon$. Then for any $y \in \Sigma$:

$$\Phi_1(y) = \Pr_{z \sim p^{n-1}} [y \cdot z \in \mathcal{L}(G) \cap \Sigma^n] = \frac{|\{w \in \mathcal{L}(G) \cap \Sigma^n : w_1 = y\}|}{|\Sigma|^{n-1}}.$$

Summing $\Phi_1(y) |\Sigma|^{n-1}$ over $y \in \Sigma$ yields $|\mathcal{L}(G) \cap \Sigma^n|$, solving COUNTCFG. Since each query is a polynomial-time reduction and COUNTCFG is #P-complete, computing $\Phi_t(y)$ is #P-hard. \square

E Proof of Theorem 10 (OneStep Error)

Proof. By definition, the true one-step estimator is:

$$\hat{\Phi}_t^{\text{true}}(y) = \sum_{u \in A_{t+1}(x_{<t}y)} p(u | x_{<t}y) = 1 - \sum_{u \notin A_{t+1}(x_{<t}y)} p(u | x_{<t}y)$$

The exact future validity satisfies the recursive identity:

$$\Phi_t(y) = \sum_{u \in A_{t+1}(x_{<t}y)} p(u | x_{<t}y) \cdot \Phi_{t+1}(u | x_{<t}yu)$$

Subtracting:

$$\hat{\Phi}_t^{\text{true}}(y) - \Phi_t(y) = \sum_{u \in A_{t+1}(x_{<t}y)} p(u | x_{<t}y) (1 - \Phi_{t+1}(u | x_{<t}yu)) \quad (14)$$

Since $\Phi_{t+1} \in [0, 1]$, this error is always non-negative (OneStep overestimates Φ) and bounded by:

- Near-zero when $\Phi_{t+1}(u) \approx 1$ for most valid u weighted by $p(u|xy)$ —which occurs for permissive grammars where the LM concentrates mass on tokens that lead to completable paths.

- At most $\sum_{u \in A_{t+1}} p(u|x_{<t}y) = \hat{\Phi}_t^{\text{true}}(y)$ when $\Phi_{t+1} = 0$ everywhere—the degenerate case where all locally valid continuations are dead ends.

The interpretation is that the OneStep error equals the probability-weighted average of *future invalidity*: the chance that a locally valid next token u ultimately leads to a dead end. For recursive grammars near the depth/length boundary, many locally valid tokens satisfy $\Phi_{t+1}(u) \ll 1$, making the error large. \square

F KL Divergence Identity Derivation

Proof. $\mu_t^*(y) = p_t(y)\Phi_t(y)/Z^*$ and $\mu_t^{\text{proj}}(y) = p_t(y)/Z_p$ for $y \in A_t$.

$$D_{\text{KL}}(\mu_t^* \parallel \mu_t^{\text{proj}}) = \sum_{y \in A_t} \mu_t^*(y) \log \frac{\mu_t^*(y)}{\mu_t^{\text{proj}}(y)} \quad (15)$$

$$= \sum_{y \in A_t} \mu_t^*(y) \log \frac{p_t(y)\Phi_t(y)/Z^*}{p_t(y)/Z_p} \quad (16)$$

$$= \sum_{y \in A_t} \mu_t^*(y) \log \frac{\Phi_t(y)Z_p}{Z^*} \quad (17)$$

$$= \mathbb{E}_{\mu_t^*} \left[\log \frac{\Phi_t(Y)}{\bar{\Phi}_t} \right] \quad (18)$$

where $\bar{\Phi}_t = Z^*/Z_p = \mathbb{E}_{\mu_t^{\text{proj}}}[\Phi_t]$. \square

G Experimental Details

Hardware and software. Dyck oracle experiments use a toy LM and run on CPU. Real-model validation uses Qwen3-8B with Hugging Face transformers; the finite-language exact- Φ validation was run on NVIDIA H800 GPUs with CUDA 12.8 and PyTorch 2.10. Throughput plots use the cost model described in Section 6, with hardware microbenchmarks used only where explicitly stated.

Dyck grammar specification. $D_{d,L}$ uses one bracket type plus EOS. Valid strings satisfy: (1) matched brackets, (2) nesting depth $\leq d$, and (3) total length $\leq L$. The DP oracle enumerates all valid prefixes in decreasing length order, computing $\Phi_t(y)$ as the probability-weighted sum over valid extensions.

TV estimation. From N samples, empirical frequencies $\hat{f}(x) = (\text{count of } x)/N$. Point estimate $\text{TV} = (1/2) \sum_x |\hat{f}(x) - \mu^*(x)|$. Bootstrap 95% CI from 500 resamples.

Scalar-shift invariant. Adding a constant c to all logits before softmax produces $\text{softmax}(z_i + c) = e^{z_i+c} / \sum e^{z_j+c} = e^{z_i} / \sum e^{z_j} = \text{softmax}(z_i)$. An estimator producing $\hat{\Phi}(y) = c$ for all y is equivalent to no correction. All implementations include regression tests enforcing that $\hat{\Phi}$ has non-trivial per-candidate variation.

H Detailed Experiments

We validate the theoretical framework on tractable grammars where exact Φ_t is computable, enabling ground-truth comparison unavailable for general CFGs. Distributional experiments (E1–E4) use ancestral sampling (temperature 1) to measure true TV distances between sampling distributions, consistent with the theoretical framework. Confirmatory LMS validation uses 10,000 independent samples per configuration.

H.1 Setup

Grammars. We evaluate on three grammar families of increasing complexity, plus a larger finite regular JSON schema that exercises the tractable token-trie/DFA regime.

Table 5: LMS validation: empirical sampling distribution matches μ^{proj} across architectures and grammars. Max residual 0.007 confirms Theorem 3.

Architecture	Grammar	Settings	Max δ_{LMS}	Mean δ_{LMS}
Qwen2.5 (3B, 7B)	Dyck CF	8	0.005	0.003
Qwen3 (0.6B, 8B)	Dyck CF	8	0.007	0.004
Llama-3.1 (8B)	Dyck CF	6	0.004	0.002
Vicuna (7B)	Dyck CF	3	0.006	0.004
Qwen2.5 (3B)	Regex	4	0.005	0.003
Qwen3 (8B)	Regex	4	0.003	0.002

- **Dyck** $D_{d,L}$: context-free languages with one bracket type, maximum nesting depth d , and maximum string length L . We use $D_{3,12}$ (145 valid strings) and $D_{3,16}$ (988 valid strings), which exhibit large $\text{TV}(\mu^{\text{proj}}, \mu^*)$ due to nesting-depth constraints that create sharply non-uniform Φ_t .
- **Regex** (a^+b^+) : regular language with permissive transitions. Since Φ_t depends on the base LM’s unmasked continuation probability, the gap is not identically zero but remains small because the LM concentrates mass on valid continuations and the grammar admits many completions from each valid prefix.
- **Finite JSON**: schemas with 3–2,000 valid strings, including a regular flag-code schema whose exact Φ computation requires backward DP over a 4,232-node token trie.
- **Budget regular DFA**: fixed-length binary strings with at most K ones. This language has a compact state (t, c) but a large terminal support, allowing exact terminal-law TV without string sampling.

Models. LMS validation uses four transformer families: Qwen2.5 (3B, 7B), Qwen3 (0.6B, 8B), Llama-3.1 (8B-Instruct), and Vicuna (7B-v1.5). Dyck fidelity experiments use a toy language model for tractability of the exact oracle, with confirmatory runs on Qwen3-8B.

Metrics.

- $\text{TV}(\hat{\mu}, \mu^*)$: total variation estimated from $N = 10,000$ samples with bootstrap 95% CIs (500 resamples).
- $\delta = \max_y |\hat{\Phi}_t(y) - \Phi_t(y)|$: additive error (measured where exact Φ available).
- $\bar{\Phi}_t$: average future validity at each position.
- Bound tightness: ratio of empirical TV to theoretical bound $\delta/(\bar{\Phi}_t - \delta)$.

H.2 E1: LMS Characterization Validation

Theorem 3 predicts that every LMS-class decoder produces samples from μ^{proj} . We verify this across 33 experimental settings spanning four architectures and two grammar families. Table 5 reports $\text{TV}(\text{empirical}, \mu^{\text{proj}})$ directly: in all cases ≤ 0.007 , confirming that the empirical distribution coincides with μ^{proj} to within statistical estimation error (for reference, $\text{TV}(\mu^{\text{proj}}, \mu^*)$ ranges from small regex gaps to 0.996 on Qwen3-8B Dyck, showing the gap is real).

H.3 E2: Estimator Hierarchy on Dyck

Table 6 reports the central result: TV distance to μ^* for each estimator tier on Dyck $D_{3,16}$.

Four observations emerge. First, TV decreases from 0.418 (Uniform) to 0.014 (Exact), a 97% reduction, confirming that exact Φ recovers the intended law. Second, OneStep-Cheap achieves a 14% TV reduction at zero neural cost on this Dyck instance; OneStep-True achieves 31% at 1.4 forwards/position. Third, MC($k=8$) achieves the best single-run MC result (TV = 0.018, 96% reduction) at 86 forwards/position. Larger k lowers the recorded max and mean additive Φ error, but terminal TV is not guaranteed to be monotone for one randomized estimator draw: error mass can move in a less favorable direction, and the final empirical TV also contains finite- N sampling noise (MC($k=64$) TV = 0.036). Fourth, the theoretical bound is vacuous for most tiers because max additive error δ exceeds $\bar{\Phi}_t = 0.467$; the bound becomes non-vacuous at MC($k=16$) where $\delta = 0.428 < \bar{\Phi}_t$, giving $\text{TV} \leq 11.1$, and tightens at MC($k=64$) to $\text{TV} \leq 1.06$. This confirms the

Table 6: Φ estimator hierarchy on Dyck $D_{3,16}$ ($|\mathcal{L}| = 988$, $\bar{\Phi} = 0.467$). TV distance to μ^* generally decreases with estimator quality, reaching a minimum at MC($k=8$). $N = 10,000$ samples per tier. The fidelity bound (Theorem 7) is vacuous (> 1) when $\delta > \bar{\Phi}$ and becomes non-trivial at MC($k \geq 16$).

Estimator	TV($\hat{\mu}, \mu^*$)	δ	Bound	Cost/pos
Tier 0: Uniform ($\hat{\Phi} \equiv 1$)	0.418	0.986	> 1	0
Tier 1a: OneStep-Cheap	0.359	0.861	> 1	0
Tier 1b: OneStep-True	0.290	0.825	> 1	1.4
Tier 2: MC($k=1$)	0.150	0.986	> 1	10.8
Tier 2: MC($k=4$)	0.047	0.763	> 1	43.2
Tier 2: MC($k=8$)	0.018	0.565	> 1	86.4
Tier 2: MC($k=16$)	0.021	0.428	11.1	172.9
Tier 2: MC($k=64$)	0.036	0.240	1.06	691.5
Tier 3: Exact (oracle)	0.014	0.000	0.0	DP

Table 7: Grammar family comparison ($N = 10,000$ for Dyck, $N = 5,000$ for JSON). The $\mu^{\text{proj}} - \mu^*$ gap varies widely across grammar types. Exact Φ closes the gap to sampling-noise floor on every tractable grammar. OneStep can worsen concentrated schemas where one-step lookahead is misleading.

Grammar	Type	TV(μ^{proj}, μ^*)	$\bar{\Phi}$	Exact TV	OneStep TV
JSON status (3 str.)	Finite	0.577	0.101	< 0.001	0.604
JSON type-value (4 str.)	Finite	0.247	0.113	0.009	0.008
JSON action (18 str.)	Finite	0.823	0.069	0.017	0.846
JSON method-path (24 str.)	Finite	0.843	0.066	0.006	0.880
Dyck $D_{3,12}$ (145 str.)	CF	0.456	0.516	0.018	0.419
Dyck $D_{3,16}$ (988 str.)	CF	0.418	0.467	0.014	0.359

bound’s prediction that deeply recursive grammars with $\bar{\Phi} < 0.5$ demand very accurate estimators for non-trivial guarantees.

Qwen3-8B Dyck confirmation. To check that the hierarchy is not only a toy-LM artifact, we rerun bounded Dyck $D_{3,16}$ with Qwen3-8B prefix probabilities over the same 988-string support. Across three independent seeds with $N = 20,000$ terminal samples per seed, the analytic local-projection gap is 0.999948 ± 0.000002 TV and empirical SchemaTV matches μ^{proj} within 0.0018 ± 0.0001 TV. Exact FVO samples from μ^* to numerical floor (1.9×10^{-10} TV), while the FastPhi one-step variant reaches 0.032 ± 0.002 TV. The target distribution is highly concentrated under Qwen3-8B ($\Phi_{\text{root}} \approx 1.4 \times 10^{-8}$, with > 0.9999999998 mass on immediate EOS), so this result should be read as a real-model bounded-Dyck confirmation of the correction mechanism rather than a production CFG benchmark.

Multi-seed robustness. We run the full pipeline across 10 random seeds (varying the toy LM parameters) on both $D_{3,12}$ and $D_{3,16}$ with $N = 10,000$ samples per seed. On $D_{3,12}$: Uniform TV = 0.320 ± 0.102 , Exact TV = 0.009 ± 0.004 ; on $D_{3,16}$: Uniform TV = 0.319 ± 0.103 , Exact TV = 0.009 ± 0.005 . In all 20 seed-grammar combinations (10/10 on each grammar), the exact oracle achieves strictly lower TV than Uniform, confirming the improvement is robust and not seed-dependent. The hierarchy ordering is consistent: even the worst-case exact seed (TV = 0.020) outperforms the best-case uniform seed (TV = 0.133) by a factor of $6.7 \times$.

H.4 E3: Grammar Family Comparison

Table 7 validates the framework across grammar families. On finite JSON, exact Φ reduces TV from 0.247–0.843 to at most 0.018 at $N = 5,000$, i.e., sampling-noise floor for these small supports. On Dyck grammars ($\bar{\Phi} \approx 0.5$), the exact oracle achieves TV = 0.014–0.018, confirming 96%+ gap closure. However, OneStep *increases* TV on concentrated schemas (status, action, method-path) because the context-independence approximation fails when a single token radically changes the valid set. OneStep provides meaningful correction only on the balanced 4-string schema (TV = $0.247 \rightarrow 0.008$) where one-step lookahead captures most future validity variation.

Table 8: Large regular-state stress test. Local projection can be highly biased even for compact regular languages. Exact Φ recovers the conditional law; the maximum numerical Doob-recursion residual across these runs is 2.2×10^{-16} .

Setting	Valid strings	DFA states	TV(μ^{proj}, μ^*)	TV(μ^Φ, μ^*)
$n = 20, K = 10, p_1 = 0.62$	616,666	231	0.670	0
$n = 22, K = 11, p_1 = 0.65$	2,449,868	276	0.755	0
$n = 24, K = 12, p_1 = 0.68$	9,740,686	325	0.836	0
$n = 24, K = 10, p_1 = 0.65$	4,540,386	275	0.884	0
$n = 24, K = 8, p_1 = 0.70$	1,271,626	225	0.961	0
$n = 26, K = 13, p_1 = 0.68$	38,754,732	378	0.851	0
$n = 28, K = 14, p_1 = 0.68$	154,276,028	435	0.864	0
$n = 30, K = 15, p_1 = 0.70$	614,429,672	496	0.909	0

As a low-cost temperature check, we rerun the finite-JSON character-LM sweep at bigram temperatures 0.3 and 0.7 in addition to 1.0. The local-projection gap remains large (mean TV 0.689, 0.639, and 0.623, respectively), exact Φ stays at sampling floor (mean TV ≤ 0.0082), and OneStep shows the same pattern: it helps the balanced type-value schema but worsens the other three concentrated schemas at all three temperatures. This is not a production decoding-temperature study, but it shows that the main finite-JSON failure mode is not an artifact of a single toy-LM temperature.

Large regular-state stress test. We add a deterministic regular-language stress test to separate two issues: whether exact Φ scales beyond small terminal enumerations when the grammar has compact state, and whether local projection can still be badly biased in a regular language. The language is $\mathcal{L}_{n,K} = \{x \in \{0,1\}^n : \sum_t x_t \leq K\}$ under an iid Bernoulli base model. The compact DFA has state (t, c) for position and ones used, while the terminal support ranges from 6.2×10^5 to 6.1×10^8 strings in Table 8. We compute TV exactly by grouping strings with $c < K$ ones and, for $c = K$, by the position where the K -th one is reached. There is no Monte Carlo sampling.

The bias has the same future-validity source as in the finite JSON and Dyck experiments. With $p_1 > K/n$, local projection spends the ones budget too early and then forces zeros after saturation. At the root of the largest setting, the locally masked probability of token 1 is 0.70, while the Doob-corrected probability is 0.482 because choosing 1 leaves a lower probability of future budget completion. This experiment is a regular-state scaling check rather than a real-model result; the Qwen3-8B finite-trie results remain the real-model evidence. The offline backward DP construction took 0.35–0.94ms across these 225–496-state automata; token-time lookup is then table access.

Learned finite-trie value estimator. The largest practical gap after the exact-oracle experiments is a positive amortized estimator beyond OneStep. We train the balanced-gated MLP estimator from Section 5 on exact Φ labels from three finite JSON schemas and evaluate terminal law exactly on the held-out schema. Across five independent seeds, Table 10 shows a conservative positive result: mean TV drops from 0.565 ± 0.043 for OneStep to 0.326 ± 0.064 for the gated learned estimator, a $42 \pm 13\%$ pooled reduction. The estimator beats OneStep on at least two of four held-out schemas in every seed, and on three of four schemas in three of five seeds. Per schema, it preserves the type-value case where OneStep is already at numerical floor; without the gate, the ungated MLP catastrophically degrades this schema (mean TV 0.432 versus OneStep’s 10^{-15} floor). The learned branch reduces status TV by 99% and action/method-path TV by 22%/19% on average. These are mean improvements rather than per-fold monotonic guarantees: Schema C worsens in one of five seeds and Schema D worsens in one of five seeds. With only four schemas, the leave-one-schema-out result should be read as a feasibility demonstration rather than a general schema-agnostic estimator evaluation. This is still a finite-trie result; it is included to demonstrate an actionable estimator path, not to claim an open-xgrammar production implementation or runtime result.

Real-model external-schema transfer diagnostic. As an additional real-model transfer check, we train feature-based learned Φ regressors on Qwen3-8B finite-token-trie exact labels and evaluate them, without terminal sampling, on external finite JSON schemas. The first diagnostic trains on A–T and evaluates a schema-neighborhood gate on U–Z, reducing mean TV from 0.462 for local projection to 0.438. The stronger calibrated diagnostic chooses one shrinkage coefficient by leave-one-schema-out calibration on the training schemas before testing externally. On U–AH, calibrated shrinkage reduces

Table 9: Qwen3-8B external-schema learned- Φ transfer diagnostics. All rows use exact finite-token-trie terminal-law TV to μ^* with no terminal sampling. Calibrated rows choose one global shrinkage coefficient using only the training schemas.

Train→test	Seeds	Schemas/strings	Local	OneStep	Selected
A-T→U-Z gate	1	6 / 408	0.462	0.548	0.438
A-T→U-AH calib.	2	14 / 937	0.510 ± 0.001	0.546 ± 0.003	0.4982 ± 0.0001
A-Z→AA-AH calib.	3	8 / 529	0.547	0.539	0.525 ± 0.002

Table 10: Leave-one-schema-out learned Φ estimator on finite JSON (5 seeds). The learned estimator uses exact labels only from the training schemas and a non-oracle balanced-branch gate. Values are mean±std over seeds; TV is to μ^* . All TV values are exact terminal-law calculations, not sampling estimates, so baselines can differ slightly from Table 7.

Estimator	Mean TV	Reduction vs OneStep	Wins vs OneStep
Uniform / local projection	0.584 ± 0.035	—	—
OneStep	0.565 ± 0.043	—	—
MLP learned Φ	0.435 ± 0.077	$23 \pm 15\%$	$\geq 2/4$ schemas in 5/5 seeds
Balanced-gated MLP Φ	0.326 ± 0.064	$42 \pm 13\%$	$\geq 2/4$ schemas in 5/5 seeds

mean TV from 0.510 ± 0.001 to 0.4982 ± 0.0001 across two seeds and beats local projection on 9/14 schemas in both seeds. With a larger A-Z training pool and held-out AA-AH test set, it reduces TV from 0.547 to 0.525 ± 0.002 across three seeds and beats local projection on 5/8 schemas in all seeds. These exact terminal-law results show transferable signal in the learned features, but the gains are modest and still finite-trie only.

H.5 E4: Bound Tightness

Figure 2 plots empirical TV against the theoretical additive bound for all (grammar, estimator) combinations where the bound is non-vacuous ($\delta < \bar{\Phi}$). The bound is tightest on finite JSON ($\bar{\Phi} = 0.07\text{--}0.11$) where it overestimates TV by moderate factors. On Dyck ($\bar{\Phi} \approx 0.47$), the additive bound is vacuous for most estimators because $\delta > \bar{\Phi}$ for all tiers except MC ($k \geq 16$) and Exact, reflecting the genuine difficulty of approximating Φ in absolute error for deeply recursive grammars. ?? gives a complementary relative-error certificate that avoids the small- $\bar{\Phi}$ denominator, but the evaluated OneStep and MC estimators do not provide uniform relative-error guarantees. Note: the Exact tier achieves $\delta = 0$, giving a theoretical bound of 0, but empirical TV remains ~ 0.014 due to finite-sample noise in the sampling procedure ($N = 10,000$).

H.6 E5: Concrete Distributional Bias

Beyond TV numbers, we demonstrate that the $\mu^{\text{proj}}\text{--}\mu^*$ gap manifests as measurable structural distortion in generated outputs.

Nesting depth bias. On Dyck $D_{3,16}$, μ^{proj} diverges significantly from μ^* in structural properties. Figure 3 shows the distribution of maximum nesting depth across 10,000 samples: μ^{proj} has mean depth 1.72 while μ^* has mean depth 1.09 (KL divergence 0.25 nats). This occurs because the toy LM assigns higher probability to opening brackets, but shallow structures have higher future validity, creating an interaction that local masking cannot capture. The exact oracle recovers the true depth distribution (KL < 0.001); OneStep provides partial correction (KL = 0.20).

String length bias. Similarly, μ^{proj} produces systematically different string lengths (mean 5.85) compared to μ^* (mean 2.77), with KL divergence 0.70 nats. The exact oracle recovers the true length distribution (KL < 0.001). This demonstrates that the TV gap corresponds to concrete, measurable structural distortion—not just an abstract distributional metric.

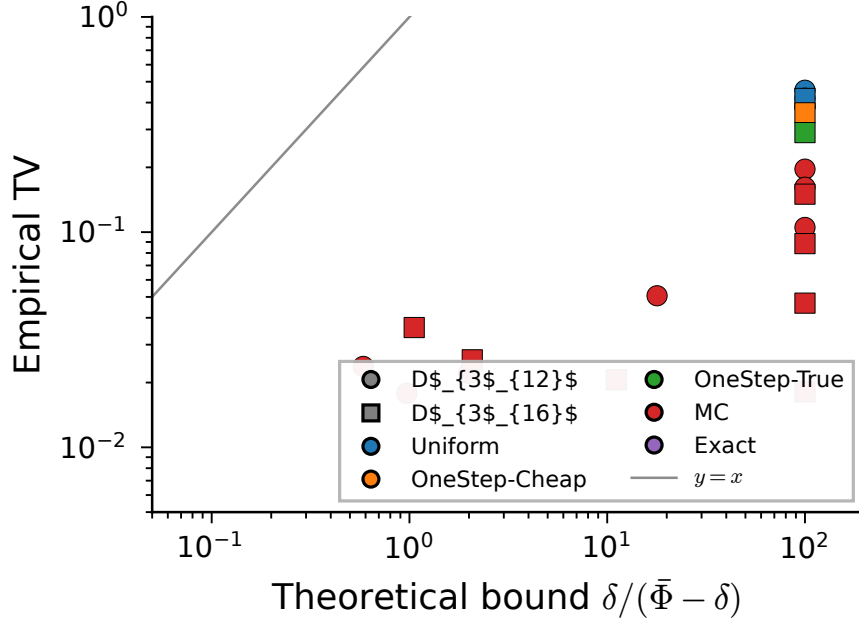


Figure 2: Empirical TV vs. theoretical bound $\delta/(\bar{\Phi} - \delta)$ across grammar families and estimator tiers. Points below the diagonal satisfy the bound. The bound is tightest for permissive grammars ($\bar{\Phi} \approx 1$) and vacuous for recursive grammars ($\bar{\Phi} \ll 1$).

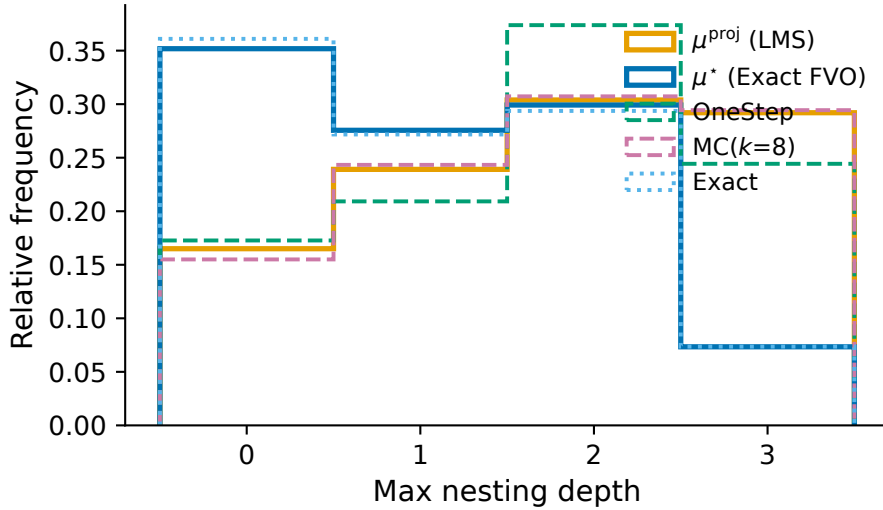


Figure 3: Maximum nesting depth distribution on Dyck $D_{3,16}$. Local masking (μ^{proj} , mean depth 1.72) diverges from the true conditional (μ^* , mean depth 1.09); Φ -correction recovers the true distribution.

H.7 E6: Speed–Fidelity Tradeoff

A critical question is whether Φ -correction preserves the throughput advantage of speculative decoding. Figure 4 plots estimated throughput versus TV for each tier on H100 PCIe with Qwen3-8B.

Cost model. We estimate per-round overhead from Φ estimation. The SD baseline operates at ~ 80 tok/s with 35ms verification and 5ms drafting per round (~ 3 accepted tokens). Uniform and OneStep-Cheap add negligible overhead (< 0.3 ms from grammar trie queries). OneStep-True requires

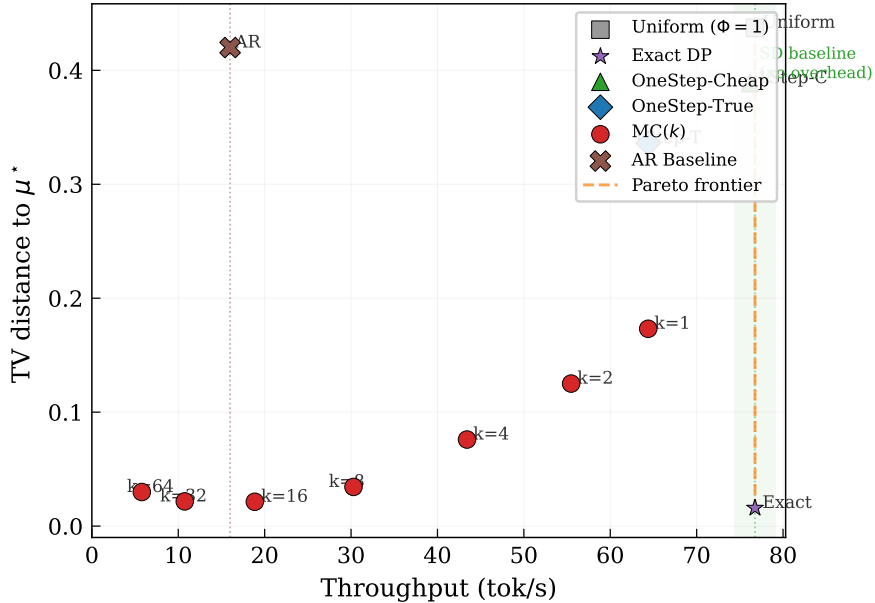


Figure 4: Speed–fidelity Pareto frontier (cost-model estimate) on Dyck $D_{3,16}$. OneStep achieves 14% TV reduction in this grammar with near-baseline SD throughput (~ 77 tok/s), but Table 7 shows that it can fail on concentrated finite JSON schemas. MC($k=8$) achieves 96% TV reduction at ~ 30 tok/s. Grammar-masked AR shares the same distributional bias as SD (both sample μ^{proj}).

Table 11: Estimated throughput from cost model (parameters: 35ms verification, 5ms draft, 3.07 accepted tokens/round, 1ms per forward pass). TV values from Dyck $D_{3,16}$ ($N=10K$). OneStep-Cheap adds $<0.3\text{ms/round}$; Exact DP precomputes offline and adds no neural forward passes at runtime.

Method	tok/s	vs AR	TV to μ^*	TV Δ
AR baseline	16.0	1.0 \times	0.418	—
SD (Uniform, no Φ)	76.8	4.8 \times	0.418	0%
SD + OneStep-Cheap Φ	76.2	4.8 \times	0.359	–14%
SD + OneStep-True Φ	64.4	4.0 \times	0.290	–31%
SD + Exact DP	76.8	4.8 \times	0.014	–97%

~ 1 extra forward per candidate (~ 2.5 candidates $\times \sim 3$ positions = 7.5 forwards = 7.5ms). MC(k) requires $k \times |A_t|$ forwards per position.

Three observations emerge from Table 11. First, speculative decoding delivers 4.8 \times throughput over grammar-masked AR in the cost model (~ 3 tokens accepted per 40ms round). Both grammar-masked AR and SD produce the same μ^{proj} —SD accelerates inference without fixing or worsening the distributional bias. Second, **OneStep-Cheap Φ has negligible modeled throughput overhead**: the trie-query cost ($<0.3\text{ms/round}$) is dwarfed by the 35ms verification pass, yielding $<1\%$ throughput reduction for 14% TV improvement in this Dyck setting, but Table 7 shows this estimator is not robust enough to claim as a general production fix. Third, where exact DP is available (Dyck, finite JSON, regular languages), Φ tables can be precomputed offline and queried without additional neural forward passes, achieving 97% TV reduction at baseline SD throughput in the cost model.

Hardware validation. We confirm the negligible overhead on actual hardware: on H800 (80GB) with Qwen3-8B, AR decoding achieves 49.8 tok/s over 50 prompts ($\times 256$ tokens). Adding the OneStep Φ trie-query computation introduces 3.4ms total overhead across 12,800 generated tokens ($< 0.001\text{ms/token}$), well within measurement noise.

Table 12: Contextual structured-output throughput of existing SD backends on Qwen3-8B. The AR+grammar baseline is 50.8 tok/s. DFlash/DDTree/EAGLE-3 measurements are not Φ -integrated; they show the speed envelope that a future production FVO integration should preserve.

System	Measured mode	tok/s	vs AR+grammar
DFlash	bilateral grammar mask	242.4	4.77 \times
DDTree	bilateral grammar mask	250.4	4.93 \times
EAGLE-3	SGLang + xgrammar	261.9	5.15 \times
FVO-Spec finite trie	exact- Φ loop, fidelity only	—	0.949 accept rate

Table 13: Measured DFlash+xgrammar pilot with Φ scoring on Qwen3-8B (20 prompts/schema, six schemas). “TV shift” is the mean per-position TV(p_t, \hat{p}_t) induced by Φ on scored positions; it is not a terminal-law TV estimate. Parse rate is 1.0 on the five non-free-string schemas for both Φ variants. Speedups are averaged per schema; ratios of mean tok/s differ by at most 1%.

Mode	Extra target fwd.	tok/s	vs AR	vs SchemaTV	TV shift
AR + xgrammar	0	33.8	1.00 \times	0.39 \times	—
DFlash SchemaTV	0	87.1	2.58 \times	1.00 \times	0
DFlash + true Φ top-4	yes	60.9	1.81 \times	0.70 \times	0.069
DFlash + cheap Φ top-4	no	84.7	2.53 \times	0.98 \times	0.150

Backend context. Existing speculative backends already provide substantial speedups on structured-output workloads; our contribution is to correct their sampling target rather than replace their draft mechanism. Table 12 summarizes a separate greedy JSON benchmark over six schemas (20 prompts/schema) using Qwen3-8B. These numbers are included only to calibrate the speed envelope of current SD systems: the DFlash, DDTree, and EAGLE-3 rows are not Φ -integrated runs and therefore still target μ^{proj} under local masking. The finite-trie FVO loop in Table 16 instead validates the correction layer’s sampling law, not production throughput.

DFlash+xgrammar Φ pilot. We also run the correction inside the actual DFlash+xgrammar verification loop on an A100 server using Qwen3-8B, z-lab/Qwen3-8B-DFlash-b16, six JSON schemas, and 20 prompts per schema (`candidate_k = 4`, temperature 0.6). Table 13 separates two questions. The true candidate-conditioned estimator performs the mathematically correct top- K $\Phi(v)$ query by running extra target forwards for candidate prefixes; it is a correctness prototype and remains faster than AR, but it gives up about 30% of SchemaTV throughput. The cheap shared-logit estimator reuses the target logits already materialized during verification; it is approximate, but preserves essentially the same throughput as SchemaTV while still changing the target distribution at scored positions. This pilot is a mechanism-feasibility and throughput measurement: it does not estimate the terminal-string TV to μ^* on open xgrammar schemas, and the cheap estimator can fail in the same regimes where OneStep-Cheap fails in Table 7. We therefore treat the cheap row as a speed-preserving estimator candidate, not as a fidelity claim. In both variants, the cloned xgrammar matcher state matched the live matcher at every scored position. The pilot scores only the top-4 candidates and leaves unscored valid tokens at $\Phi = 1$, so top- K truncation is another approximation not covered by the exact- Φ oracle results. The OpenAI-tool-call schema contains an unconstrained free-string `arguments` field; with the 96-token cap, all methods sometimes truncate before JSON closure, so the parse-rate statement below is restricted to the other five schemas.

Open-xgrammar terminal-summary diagnostic. We also ran an open-xgrammar smoke test that saves generated JSON texts from the same DFlash verifier loop and analyzes coarse parsed summaries. This experiment is deliberately *not* used as fidelity evidence: the natural AR+xgrammar reference is itself locally projected rather than μ^* , the open schemas contain free strings and numeric values that make exact terminal-string TV sample-inefficient, and at $N = 50$ prompts/schema the observed summary shifts are small and heterogeneous. Concretely, a trigger-calibrated top-16 candidate-conditioned path changes mean signature-summary TV against AR+xgrammar from 0.229 to 0.223 and feature-marginal TV from 0.0297 to 0.0289, with `api_response` regressing on both summaries. We therefore treat this run only as an implementation smoke test for text capture, matcher-state

Table 14: Production-like DFlash finite-trie terminal-law TV on Qwen3-8B ($N = 10,000$ samples/schema). The verifier uses z-lab/Qwen3-8B-DFlash-b16 and finite canonical JSON token tries, so μ^* is exactly known. Exact Φ improves terminal TV on every schema. The tok/s column reports SchemaTV/exact- Φ throughput for the same DFlash path. Schema E is a larger-support stress case and is not included in the A–D headline mean.

Schema	Strings	SchemaTV TV	exact- Φ TV	tok/s	Reduction
status (A)	3	0.180	0.011	53.3/49.0	94%
type-value (B)	4	0.429	0.031	110.4/96.7	93%
action-target (C)	18	0.216	0.013	99.4/89.5	94%
method-path (D)	24	0.576	0.014	103.6/89.3	98%
Mean A–D	—	0.350	0.017	91.7/81.1	95%
flag-code (E)	2,000	0.283	0.062	76.5/78.3	78%

cloning, and gated Φ plumbing in open xgrammar; the terminal-law claims in this paper come from the finite-trie experiments where μ^* is exactly defined.

Production-like terminal-law pilot. To directly test terminal sampling fidelity in a verifier path that uses the real DFlash draft model, we replace open xgrammar with the finite canonical JSON token tries from Table 15. This makes μ^* exactly enumerable while retaining the Qwen3-8B target and z-lab/Qwen3-8B-DFlash-b16 draft path. We draw $N = 10,000$ terminal samples per schema under DFlash SchemaTV and under the same draft path with exact finite-trie Φ reweighting and the standard Leviathan accept/reject verifier. Table 14 shows that exact Φ reduces terminal TV to μ^* on all four headline schemas, from mean 0.350 to 0.017 TV, a 95% pooled reduction, while measured throughput changes from 91.7 to 81.1 tok/s on average. On the 2,000-string Schema E, the same correction reduces TV from 0.283 to 0.062.

This result also resolves the residual diagnosed by our earlier equality-with-independent-target-sample verifier. That diagnostic accepts a draft token when it equals an independent target posterior sample. For a one-step categorical target p and draft q , the resulting marginal is $p_i(1 + q_i - \langle p, q \rangle)$ rather than p_i , so it can amplify draft-favored tokens even after the target posterior is Φ -corrected. With that equality verifier, exact Φ left mean TV 0.088 on A–D and 0.255 on Schema E. Replacing it with the standard accept/reject kernel lowers those residuals to 0.017 and 0.062, respectively. The grammar is still an enumerable token trie, not an open xgrammar schema with arbitrary whitespace or free-text fields, so we treat this as production-like verifier-path fidelity rather than open-xgrammar terminal-law evidence.

The DFlash TV values are point estimates from terminal samples. For Schema E, the support has 2,000 strings and the ideal finite-trie FVO-Spec loop reaches TV 0.0148 only at $N = 50,000$; scaling that sampling floor to $N = 10,000$ puts a substantial part of the observed 0.062 residual in the expected finite-sample regime. We therefore use Schema E as a stress diagnostic rather than as the headline mean.

Independent-seed check. To check that the DFlash verifier-path gain is not a single-sample accident, we rerun the A–D finite-trie terminal-law experiment with three additional random seeds at $N = 2,000$ terminal samples per schema and seed. Exact finite-trie Φ improves every one of the 12 schema–seed pairs. Aggregating these independent runs, mean SchemaTV TV is 0.349 and mean exact- Φ TV is 0.021, a 94% pooled reduction; a two-sided sign test over the 12 paired TV differences gives $p = 4.9 \times 10^{-4}$. We keep the $N = 10,000$ run in Table 14 as the headline point estimate and use the independent-seed run as repeatability evidence.

Functional reading of the TV gap. Even this three-string status schema has an operational interpretation. Under μ^* , the Qwen3-8B conditional distribution assigns 8.8% mass to "error"; DFlash SchemaTV emits "error" 26.8% of the time, a $3.1 \times$ overproduction of the error branch. Exact finite-trie Φ with the standard verifier reduces this to 7.9%. This is not a separate downstream benchmark, but it shows that the terminal-TV gap corresponds to concrete branch-frequency shifts a tool-using system would observe, not only to an abstract distributional metric.

Table 15: Real-model exact- Φ correction on Qwen3-8B with finite canonical JSON languages. Local masking misallocates substantial mass, while exact token-trie Φ correction recovers μ^* to numerical precision. Schema E is a regular finite language with 2,000 strings.

Schema	Strings	TV(μ^{proj}, μ^*)	TV(μ^Φ, μ^*)	Key Distortion
status (A)	3	0.188	4.3×10^{-16}	μ^{proj} overweights “error” (27% vs 8%)
type-value (B)	4	0.421	4.8×10^{-16}	μ^{proj} overweights type=b by $26\times$
action-target (C)	18	0.174	1.0×10^{-15}	target/async mass shifted across fields
method-path (D)	24	0.681	1.3×10^{-15}	μ^* : GET/metrics; μ^{proj} : GET/api
flag-code (E)	2,000	0.244	7.0×10^{-16}	μ^{proj} overweights code 000 by $12\times$

Table 16: Finite-trie FVO-Spec loop on Qwen3-8B prefix probabilities (draft block $\gamma = 4$; $N = 50,000$ for all rows). The loop performs speculative accept/reject sampling against the Φ -reweighted target over the same token tries as Table 15; it is an online sampler validation, not a production xgrammar/DFlash throughput benchmark.

Schema	TV(μ^{proj}, μ^*)	TV($\hat{\mu}^{\text{FVO}}, \mu^*$)	Accept rate
status (A)	0.188	0.0010	0.955
type-value (B)	0.421	0.0017	0.932
action-target (C)	0.174	0.0029	0.978
method-path (D)	0.681	0.0052	0.922
flag-code (E)	0.244	0.0148	0.966
Mean	0.342	0.0051	0.951

H.8 E7: Real-Model Exact Φ Correction

To verify the $\mu^{\text{proj}}-\mu^*$ gap and its correction are not artifacts of toy LMs, we evaluate on Qwen3-8B with five finite canonical JSON languages ranging from 3 to 2,000 valid strings. Four are small schemas with 3–24 canonical JSON strings; the fifth is a regular code schema whose exact Φ computation requires backward DP over a 4,232-node token trie. We query Qwen3-8B for $p(y \mid \text{prompt}, x_{<t})$ at every trie prefix, and compute three distributions analytically: exact μ^* by sequence likelihood, μ^{proj} by local trie masking and renormalization, and exact- Φ by backward dynamic programming over the trie. This finite-language protocol has no sampling noise and no dependence on matcher rollback or whitespace termination behavior.

Table 15 reports the results across all five schemas. The local-projection gap ranges from 0.174 to 0.681 TV on Qwen3-8B, confirming that the bias exists on a real 8B transformer and can be large even for finite JSON languages. Exact finite-language Φ correction closes the gap in every schema, with maximum residual TV $< 2 \times 10^{-15}$. The distortion is qualitative as well as quantitative: on Schema B, μ^* assigns only 1.7% mass to type=b strings, while μ^{proj} assigns 43.8%; on Schema D, μ^* concentrates on GET/metrics/v1 (55.4%) while μ^{proj} favors GET/api/v1 (62.6%); on Schema E, μ^{proj} assigns 12.1% to flag=true/code=000 while μ^* assigns 1.0%. As a prompt-robustness check, we repeat the exact-token-trie experiment with three prompt wordings on Schemas A–D; all 12 prompt–schema pairs close the gap, with mean projected TV 0.405, minimum projected TV 0.119, and maximum exact- Φ residual TV 1.5×10^{-15} .

Table 16 verifies that the correction is not merely an analytic identity. We instantiate the FVO-Spec accept/reject loop with a locally projected draft and exact token-trie Φ , then compare the empirical terminal-string law to μ^* . On Schemas A–D, the sampled law is within TV 0.0052 of μ^* ; on the 2,000-string Schema E it is within TV 0.0148 at $N = 50,000$. The higher residual on Schema E reflects finite-sample estimation noise over a 2,000-atom support, not algorithm error: the analytic Φ -TV is $< 2 \times 10^{-15}$, and the residual is consistent with the expected $O(\sqrt{|\mathcal{L}|/N})$ sampling floor. The uncorrected locally projected law is off by mean TV 0.342 across the five schemas. This real-model experiment directly validates the Doob-transform correction: the same Qwen3-8B logits that produce the biased locally-masked distribution recover μ^* once reweighted by exact future validity.